Spectroscopic Results From Blue Hills Observatory of the 2009–2011 Eclipse of ε Aurigae

Stanley A. Gorodenski
9440 East Newtown Avenue, Dewey, AZ 86327; stanlep@commspeed.net

Received February 7, 2012; revised February 17, 2012; accepted February 28, 2012

Abstract The purpose of this paper is to report spectroscopic results of ε Aurigae during the 2009–2011 eclipse. Spectra of the sodium D lines and an absorption line occurring at approximately 5853Å were taken from February 13, 2010, to October 10, 2011, with an LHIRES III spectrograph and a 16-inch Meade telescope at Blue Hills Observatory in Dewey, Arizona. Equivalent width and radial velocity data support the presence of a void or ring structure within the eclipsing disk, and they support a central disk clearing around an unseen primary central object. The results also indicate the disk does not end at fourth contact but continues for a significant distance. Analysis of radial velocities demonstrated the profile of the 5853Å line has a disk component in addition to the primary F0 star component. A split line at this location was observed. From the equivalent width profile of the 5853Å line the duration of the split line event was estimated to be 101 days. Other lesser results are presented and discussed.

1. Introduction

ε Aurigae is an eclipsing binary system with a period of 27.1 years and an eclipse that lasts almost two years. The primary star is an F0 star although recent work indicates it may be a highly evolved object (Leadbeater 2011). The eclipse is thought to be caused by a disk of dust rotating around an unseen central object which is in orbit around the primary F0 star. The last eclipse and campaign was 1982–1984. For the 2009–2011 eclipse an international campaign was organized by Dr. Robert E. Stencel and Jeffrey L. Hopkins. There is a major difference between this campaign and the previous one. A lot of the amateur contribution to the previous campaign was in the form of electronic photometry. Since then a range of high performance CCD cameras have become available to the amateur, as well as relatively inexpensive high resolution spectrographs such as SBIG's SGS spectrograph and Shelyak's LHIRES III and eShel spectrographs. The author owns an LHIRES III spectrograph with a resolution greater than 18,000. At the encouragement of Jeff Hopkins, the author worked on the sodium D absorption lines for this campaign.

This paper consists primarily of observations and analyses with some discussion and interpretation. Although the sodium D absorption lines from the disk are confounded with absorption lines from the primary F0 star, no attempt was made to subtract the F0 contribution from the spectra. Doing so requires an out-of-eclipse estimate of the F0 absorption lines. This can be done, but using it requires one to assume the F0 radial velocities and equivalent widths do not change during the eclipse. The author prefers not to make this assumption and so an out-of-eclipse component was not subtracted. Because such a subtraction would have involved a constant component in any event, it is felt one can still obtain meaningful results and interpretations. In addition to the sodium D lines, this paper also includes a line located at approximately 5853Å. An evaluation of an out-of-eclipse spectrum taken in July 2008 by Olivier Thizy has not been successful in identifying this line. One possibility is Barium II. (The profile is 20080727-031309-epsAur-5x300s_P_1C_FULL.fit and is found at the ε Aur spectral database maintained by Robin Leadbeater at http://www.threehillsobservatory.co.uk/astro/epsaur_campaign/epsaur_campaign_spectra_table.htm.) In lieu of a definite identification, it will be referred to as the 5853Å line in this paper. It exhibits an unexpected line split which will be discussed.

The sodium doublet consists of two lines, D_2 (λ = 5889.95Å) and D_1 (λ = 5895.924Å). Figure 1 is a typical spectrum, normalized, of the sodium D lines region, about 175 Ångstroms wide, taken on February 26, 2010. Figure 2 contains profile examples to illustrate the evolution of the D lines. It also illustrates the resolution capabilities of the LHIRES III spectrograph.

The data contained in Tables 1, 2, 3, and 4, are available for download from the AAVSO ftp site at ftp://ftp.aavso.org/public/datasets/jgoros402a.txt, jgoros402b.txt, jgoros402c.txt, and jgoros402d.txt.

2. Instrumentation and methods

The work was conducted at the author's personal observatory, Blue Hills Observatory (http://users.commspeed.net/stanlep/homepagens.html), located in Dewey, Arizona. The equipment consisted of a Meade 16-inch LX200R telescope (vintage 2006), the LHIRES III spectrograph, an ST8-XME camera for imaging the spectra, and a Meade DSI I camera for guiding. The spectrograph's slit width was set at 22-microns, which enabled the spectrograph to obtain higher resolution spectra than possible with the wider width, usually around 30 to 35 microns, normally used by owners of the LHIRES. Various guiding software was tried and tested. The major ones used were Meade's ENVISAGE and PHD. CCDSOFT captured the images, IRIS (version 5.57) was used to reduce the spectra, and VSPEC and AUDELA were used to calibrate and do additional processing. Great care was taken to obtain very good calibrations using telluric lines. After calibration the telluric lines were removed (using VSPEC) and the spectra were then heliocentric corrected. After all this processing, the reduced spectra were analyzed using SPSS, a statistical software package. The graphs and tables in this paper were produced with SPSS.

Table 1 gives the dates the spectra were taken. Because of the short integration time—only ten minutes—many times more than one spectrum per night were obtained. The result was a total of seventy spectra over the time period the author participated in the campaign. The data points of these additional spectra per night can be seen in the graphs in this paper.

3. Equivalent width

Equivalent width (EW) was estimated using the method described by Gorodenski (2011). With this method a continuum is estimated with a least squares polynomial regression model. The beginning and end points of a line for the purpose of computing an EW are defined where the line is judged to come in contact with, or cross through, the estimated continuum. At times during the evolution of the Na D lines, the midpoint between the D_2 and D_1 lines drops below the estimated continuum. When this happened the crossover points for estimating the equivalent widths were taken to be midway between the D lines.

Table 1 has the equivalent widths (in Ångstroms) and 95% upper and lower confidence limits for the Na D lines and the 5853Å line. Figures 3 and 4 are plots of the equivalent widths of the Na D_2 and Na D_1 lines, respectively.

The estimated contact dates of the eclipse in B band from Hopkins (2012) are:

1st Contact	August 11, 2009	JD 2455054
2nd Contact	December 19, 2009	JD 2455184
Mid-Eclipse	August 4, 2010	JD 2455412
3rd Contact	March 19, 2011	JD 2455639
4th Contact	May 13, 2011	JD 2455694

The applicable dates (the last three) are shown in all the graphs in this paper.

The disk inclination has been reported to be nearly edge on (Hopkins and Stencel 2008) and at most 90° ± 2° (Kloppenborg 2012). As the disk moves across (eclipses) the star, the amount of disk material contributing to a spectrum should be at a minimum at mid-eclipse, gradually increase to a maximum at third contact, and after third contact it should decline. One would expect equivalent widths to conform to these changing amounts of disk material. The profile of the equivalent widths in Figures 3 and 4 generally agrees with these expectations. The equivalent widths are at a low point (although not the lowest as will be shortly discussed) at mid-eclipse, and they gradually increase after mid-eclipse until they reach a high point at third contact. After third contact they exhibit a decline as expected. However, the decline appears to continue well after fourth contact (150 days beyond fourth contact) when the primary F0 star should be far clear of the disk. The relatively constant slope of the decline for 150 days after the star reached fourth contact indicates the disk material does not abruptly end at this point, but gradually disappears.

There are a few irregularities in the graphs that appear to be real, that is, they are not a sampling error or a problem with the data. One is a dip at approximately January 16, 2011. The author interprets this as a variation in the amount of disk material, meaning the disk material is not distributed uniformly across the disk and may be patchy or clumpy. This agrees with Leadbeater *et al.* (2011) who interpret structure within the disk as being responsible for the rate of increase of EW during ingress.

The other anomaly, a major one, is at the beginning of the series. The series (profile) of equivalent widths start at a significantly lower level than at mid-eclipse. There is a definite increasing trend that starts from the beginning of the series and peaks on March 28, 2010. (Based on the author's experience with regression analysis, a statistically significant polynomial regression model would fit this part of the series. It should be obvious to the reader that this trend is not random error.) This anomaly over the same time period is also seen in the radial velocity graphs of D_2 and D_1 in Figures 6 and 7, respectively, in the section to follow on radial velocities.

The EW and radial velocity data together are evidence of a ring structure to the disk (Leadbeater and Stencel 2010; Seebode *et al.* 2011), or a large void in the disk (the author's hypothesis). If a ring gap or void exists, there would be less material contributing to a line strength and, hence, the equivalent width would be smaller in value. As the disk moves from first contact to the point where the primary F0 star just clears the inner boundary of the disk, radial velocities should increase, not drop, according to Kepler's Law of Planetary Motion. A large void or ring gap explains the drop in radial velocities for the following reason. Because there would be no disk material in this space there would be no disk material moving in a radial direction away from the observer (the radial velocity values are positive and so the movement would be away from the observer). The contribution to the observed radial velocities then can only come from the parts of the disk on either side of the void. What the observer sees is the radial component (the other component is the proper motion component) of the disk as it rotates. This radial component has a smaller velocity value than material moving directly away from the observer would have at the location of the hypothesized void or ring gap. As the void or gap moves across the primary F0 star, radial velocities start increasing as dust material moves into the line of sight.

Figure 5 is a graph of the 5853Å line equivalent widths. It can be seen that the EW profile is much more variable. However, a second order polynomial regression model, shown in the graph, was statistically significant at the 0.001 level, indicating the 5853Å line profile generally follows the same trend as the Na D lines. (A second order polynomial was statistically significant for both D lines and in the same direction as the 5853Å polynomial but is not displayed in the graphs because of a concern of too much graph clutter.) The large drop that bottoms out between third and fourth contact can be explained by a split line which will be discussed later.

4. Radial velocity and the 5853Å split line

An estimate of radial velocity requires an estimate of the center of a spectral line. Four different kinds of estimates were made with the assistance of VSPEC. They fall into two major categories: EW versus Visual. EW means that the beginning and end points of a line for line center estimation were the same beginning and end points that were used for estimating the line's equivalent width (using the method described in Gorodenski 2011). Because of the frequent occurrence of a long wing on the blue side of the D_2 line, it was felt this method might not give good line center estimates. Therefore, a separate set of estimates was made based on a visual "guess" of the beginning and end points of the lines in VSPEC. An attempt was made to minimize inclusion of asymmetric long wings. Although this Visual estimate is difficult to define, an attempt was made to be as consistent from spectrum to spectrum as much as possible.

Within each of these two categories, that is, EW and Visual, two kinds of line estimates were performed in VSPEC. One was a barycenter line estimate, which will be called "Barycenter," produced by checking a box in VSPEC called "Line Center." The other is a "Gaussian fit" estimate. However, VSPEC uses the line location of the barycenter of the Gaussian fitted line as the line center, that is, the line center estimate is not the estimated parameter of the Gaussian function. However, it will still be called the "Gaussian" estimate.

The line center estimates of each of the sodium D lines consisted of the four types just described. However, the 5853Å line is much weaker than the D lines. Because of this it was felt getting a "Visual" estimate for the 5853Å line would have been very difficult, maybe impossible to consistently estimate. As a result, the beginning and end points for estimating a line were the beginning and end points that were used to estimate the equivalent widths. Consequently, there were only two estimates (in contrast to the four for the D lines), the Barycenter and the Gaussian estimates.

A decision had to be made as to which of the four estimates for sodium and the two for the 5853Å line are the best for computing radial velocities. To do this a standard deviation was computed for each of the line estimation methods for each element line. Table 2 contains these standard deviations. For the 5853Å line the Barycenter estimates have a lower standard deviation than the Gaussian estimates. Hence, the Barycenter estimates were used for computing the 5853Å radial velocities. For both sodium D lines the "Visual" estimates have smaller standard deviations than the "EW" estimates. Within "Visual," the Barycenter estimates have smaller standard deviations. Hence, for the D lines the Visual-Barycenter estimates were used to compute radial velocities. Table 3 contains the line center estimates for all three lines. Table 3 also contains a VSPEC estimate of the line centers of the 5853A split line, the split line mentioned in the introduction of this paper.

Table 4 contains the radial Velocities (km/sec) for Na D_2, Na D_1, 5853Å, and the 5853Å split line. By convention, a positive value indicates a red Doppler shift, that is, the object is moving away from the observer. A negative value means a blue Doppler shift, or an object moving toward the observer.

Figures 6 and 7 are plots of the radial velocities for Na D_2 and Na D_1, respectively, with a statistically significant (0.001) 2nd order polynomial regression line for each. There are a number of things to notice. First, at mid-eclipse it is expected that the radial velocity should be equal to zero. The horizontal solid line is the zero radial velocity line. The estimated points where the interpolated Na D_2 and Na D_1 lines cross the horizontal zero radial velocity line are August 8, 2010, and August 4, 2010, respectively.

However, these are not mid-eclipse estimates because the ε Aur system is moving toward Earth at about 2.5 km/sec, ± 0.9 km/sec. Consequently, what might be a red shift radial velocity of 2.5 km/sec with ε Aur as the frame of reference will appear as a zero km/sec radial velocity from Earth, that is, with Earth as the frame of reference. Therefore, 2.5 km/sec has to be added to the radial velocities in this paper to convert to the ε Aur frame of reference. When this is done, the author's data suggest the mid-eclipse dates for Na D_2 and Na D_1 are August 18, 2010, and August 16, 2010, respectively. Because there is no quantum explanation that could allow the D line to have different mid-eclipse dates, these dates can be taken as independent estimates of the actual mid-eclipse date. Averaging the two gives an estimated mid-eclipse date of August 17, 2010.

The increasing radial velocities from the beginning of the series to March 28, 2010, have already been explained as being due to a possible ring gap, or a possible void in the disk.

The radial velocity curve from about May 6, 2010, to about November 1, 2010, in both Figures 6 and 7 supports the hypothesis that the disk has a central clear area around an unseen central object. In other words, the disk has an outer and inner edge, or boundary. Based on this hypothesis, one would expect a decreasing radial velocity from March 28, 2010 (assuming this part of the curve is at or near the inner boundary on the ingress side of the disk) to mid-eclipse and then an increasing one from mid-eclipse to November 1, 2010 (assuming this part of the curve is at or near the inner boundary on the egress side of the disk) and this is what is observed. The explanation for this expectation is the same as the one given to explain the drop in radial velocities in the above section on equivalent width. Essentially, without central dust, the observer is seeing the disk on both sides of the void. As a result, what is being observed is the radial component (the other component being the proper motion component) to the rotational motion of the disk. As the mid-eclipse is approached this radial component becomes smaller, eventually going to zero. The reverse occurs on the other side of mid-eclipse. This explains the shape and direction of the line between these dates.

As can be seen in Figures 6 and 7, the radial velocities still have not reached the zero radial velocity level after 4th contact. The last data point in the graph is October 10, 2011. This is 150 days past fourth contact. By this time the primary F0 star should be well clear of the disk. Yet, radial velocities on this date are over 8 km/sec (see Table 4). This is additional evidence in support of the EW data that the disk continues well beyond fourth contact.

Figure 8 is the radial velocity plot for the 5853Å line. It is of interest to determine whether this line is undergoing the same radial velocity change as the Na D lines. If it is, then this would be evidence there is a disk component to the 5853Å absorption line. The second order polynomials in Figures 6 and 7 for the D lines are statistically significant (0.001). Although the 5853Å radial velocities exhibit more variability than those of the Na D lines, a statistically significant (0.001) second order polynomial model also fits the data and is in the same direction as the D lines polynomials. This is evidence that there is a disk component to the 5853Å absorption line. However, this is not certain. It could all still be from the primary F0 star.

There is one big difference in the 5853Å line profile compared to the D lines. Starting just after January 27, 2011, the 5853Å radial velocities undergo a large blue shift drop and reach a high of 28.866 km/sec on April 13, 2011 (spectrum number 1 in Table 4). The Na D lines do not exhibit such a drop. The largest blue shift for the D_2 and D_1 lines were 23.842 km/sec and 23.843 km/sec, respectively, on January 17, 2011 (spectrum number 1 in Table 4).

The large drop in the 5853Å radial velocities is caused by the confounding effect of the 5853Å split line. Figure 9 is a graph of the split line radial velocities with a superimposed statistically significant (0.001) first order polynomial regression line. It can be seen the split line radial velocities had already started dropping on January 17, 2011, and reached a high blue shift of 27.954 km/sec on April 26, 2011 (spectrum number 1 in Table 4). These dates do not exactly match those for the 5853Å line but are close. There are two reasons for the inexact match: the split line data is very incomplete, and the line centers could only be roughly estimated in VSPEC. Figure 10 shows the evolution of the split line and illustrates some of the difficulties of getting line center estimates. The profile on December 25, 2010, was included to demonstrate the latter. This profile exhibits what might be called a plateau, not a well defined line such as the one on March 28, 2010.

Such a plateau makes it impossible to estimate a split line center. In addition, there were undoubtedly 5853Å spectra that contained the effects of a split line on EW and radial velocity, but the effect was too small to be noticeable in a line profile.

The start and end dates of the split line phenomenon cannot be determined from the split line data itself, but it appears a reasonable estimate might be obtained from Figure 5, the graph of the 5853Å equivalent widths. A visual inspection of the graph places the start and end of the split line at January 27, 2011, and May 8, 2011, respectively, which gives a duration of 101 days. Kim (2008) reports a 67-day and a 123-day period, although it is not clear what these periods represent, that is, what they are periods of.

5. Conclusion

This paper has demonstrated the high resolution spectroscopic work that can be done with the LHIRES III spectrograph. The paper also demonstrated the following:

1. The profile of the equivalent widths for the Na D lines generally agree with expectations prior to mid-eclipse, at mid-eclipse, and at third contact.

2. The equivalent width data for the D lines support the hypothesis that some of the variation in EW are the result of a non-homogeneous disk, that is, a disk that is patchy or clumpy.

3. The EW data support the hypothesis that the disk does not abruptly end at fourth contact, but gradually trails off.

4. The estimated mid-eclipse date based on the sodium D lines is August 17, 2010. This estimate does not differ substantially from the projected mid-eclipse date (made prior to mid-eclipse) of August 4, 2010.

5. The Na D_2 and D_1 radial velocities reached their highest value, a blue shift, of 23.842 km/sec and 23.843 km/sec, respectively, on January 17, 2011.

6. The EW and radial velocity data support the hypotheses of a ring structure to the disk as others have proposed. The author proposes as an alternative a large void within the disk.

7. The 5853Å line radial velocity profile supports the hypothesis that the 5853Å absorption line has a disk component.

8. The radial velocity data supports the existence of a central clearing around the unseen primary object of the disk, that is, the disk has an inner boundary.

9. The 5853Å absorption profile contains a split line. The estimated duration of the split line event was estimated to be 101 days.

6. Acknowledgements

I would like to thank Jeff Hopkins for encouraging me to join the ε Aur Campaign, and for encouraging me to concentrate my spectroscopy on the sodium D lines region. I would also like to thank Jeff Hopkins for suggesting that I purchase the Meade 16-inch LX200R telescope way back in the year 2005.

It has turned out to be a superb telescope for doing spectroscopy. Without his suggestion I might still be attempting to retrofit my old 12.5-inch Dall-Kirkham, made by a machinist friend, instead of participating in this campaign.

References

Gorodenski, S. 2011, *Soc. Astron. Sci. Newsl.*, **9** (no. 2), 5.

Hopkins, J. L. 2012, ε Aur Campaign website (http://www.hposoft.com/EAur09/Starinfo.html).

Hopkins, J. L., and Stencel, R. E. 2008, *Epsilon Aurigae: a Mysterious Star System*, Hopkins Phoenix Observatory, Phoenix, Arizona.

Kim, H. 2008, *J. Astron. Space Sci.*, **25**, 1.

Kloppenborg, B. 2012, private communication.

Leadbeater, R. 2011, "The International Epsilon Aurigae Campaign 2009–2011. A Description of the Campaign and early Results," arXiv:1101.1435v1 [astro-ph.SR), 67.

Leadbeater, R. 2012, ε Aur spectral database (http://www.threehillsobservatory.co.uk/astro/epsaur_campaign/epsaur_campaign_spectra_table.htm), profile 20080727-031309-epsAur-5x300s_P_1C_FULL.fit.—

Leadbeater, R., and Stencel, R. E. 2010, "Structure of the Disc of Epsilon Aurigae: Spectroscopic Observations of neutral Potassium during Eclipse Ingress," arXiv:1003.3617v2 [astro-ph.SR].

Leadbeater, R., *et al.*, 2011, *Bull. Amer. Astron. Soc.*, **43**, 257.04.

Seebode, S., Howell, S. B., Drumheller, D., Stanford, D., Hoard, D. W., and Stencel, R. E. 2011, *Bull. Amer. Astron. Soc.*, **43**, 257.08.

Table 1. ε Aur, equivalent widths (in Ångstroms) and 95% confidence limits for Na D_2, Na D_1, and the 5853Å line.

Date	*Spectrum Sequence Number*	*Julian Date*	*Na D_2 Lower Conf. Limit (Å)*	*Na D_2 EW (Å)*	*Na D_2 Upper Conf. Limit (Å)*	*Na D_1 Lower Conf. Limit (Å)*	*Na D_1 EW (Å)*	*Na D_1 Upper Conf. Limit(Å)*	*5853Å Lower Conf. Limit (Å)*	*5853Å EW (Å)*	*5853Å Upper. Conf. Limit (Å)*
2010 Feb 13	1	2455240.719352	1.2852	1.3219	1.3587	1.2008	1.2282	1.2555	.0630	.0723	.0815
2010 Feb 13	2	2455240.740081	1.2853	1.3208	1.3564	1.2034	1.2298	1.2562	.0571	.0695	.0820
2010 Feb 13	3	2455240.762222	1.2849	1.3211	1.3573	1.1979	1.2310	1.2641	.0493	.0638	.0782
2010 Feb 14	1	2455241.686528	1.3072	1.3394	1.3717	1.2141	1.2398	1.2656	.0562	.0671	.0780
2010 Feb 14	2	2455241.712986	1.2986	1.3223	1.3459	1.2075	1.2278	1.2481	.0600	.0702	.0804
2010 Feb 14	3	2455241.734444	1.2928	1.3185	1.3442	1.1967	1.2224	1.2481	.0596	.0702	.0808
2010 Feb 19	1	2455246.633507	1.2978	1.3317	1.3656	1.1997	1.2304	1.2612	.0624	.0774	.0924
2010 Feb 19	2	2455246.651863	1.2860	1.3328	1.3795	1.2034	1.2436	1.2839	.0608	.0772	.0937
2010 Feb 19	3	2455246.669815	1.2920	1.3303	1.3685	1.2072	1.2367	1.2662	.0618	.0773	.0928
2010 Feb 19	4	2455246.680093	1.3037	1.3335	1.3632	1.2095	1.2338	1.2582	.0597	.0757	.0916
2010 Feb 26	1	2455253.654190	1.2845	1.3147	1.3449	1.1939	1.2233	1.2526	.0555	.0690	.0826
2010 Mar 04	1	2455259.650289	1.2957	1.3247	1.3536	1.2032	1.2331	1.2631	.0422	.0560	.0698
2010 Mar 04	2	2455259.669225	1.2936	1.3296	1.3655	1.2038	1.2345	1.2651	.0427	.0610	.0792
2010 Mar 04	3	2455259.689699	1.3073	1.3377	1.3681	1.2043	1.2302	1.2561	.0382	.0512	.0642
2010 Mar 13	1	2455268.681319	1.3237	1.3548	1.3858	1.2273	1.2526	1.2780	.0279	.0417	.0555
2010 Mar 13	2	2455268.702488	1.3281	1.3626	1.3971	1.2318	1.2652	1.2986	.0281	.0390	.0498
2010 Mar 13	3	2455268.722338	1.3240	1.3727	1.4215	1.2292	1.2636	1.2979	.0260	.0413	.0566
2010 Mar 28	1	2455283.653206	1.4154	1.4482	1.4810	1.3029	1.3336	1.3642	.0192	.0324	.0456
2010 Mar 28	2	2455283.674873	1.4202	1.4623	1.5043	1.3112	1.3409	1.3706	.0160	.0359	.0558
2010 Mar 28	3	2455283.695197	1.4281	1.4615	1.4948	1.3269	1.3565	1.3860	.0228	.0385	.0543
2010 May 08	1	2455324.636933	1.3779	1.4161	1.4543	1.2704	1.3028	1.3351	.0464	.0622	.0781

Table continued on following pages

Table 1. ε Aur, equivalent widths (in Ångstroms) and 95% confidence limits for Na D_2, Na D_1, and the 5853Å line, cont.

Date	*Spectrum Sequence Number*	*Julian Date*	*Na D_2 Lower Conf. Limit (Å)*	*Na D_2 EW (Å)*	*Na D_2 Upper Conf. Limit (Å)*	*Na D_1 Lower Conf. Limit (Å)*	*Na D_1 EW (Å)*	*Na D_1 Upper Conf. Limit(Å)*	*5853Å Lower Conf. Limit (Å)*	*5853Å EW (Å)*	*5853Å Upper. Conf. Limit (Å)*
2010 May 08	2	2455324.647917	1.3813	1.4145	1.4477	1.2697	1.2976	1.3256	.0496	.0655	.0814
2010 May 08	3	2455324.658241	1.3788	1.4215	1.4642	1.2599	1.2959	1.3319	.0527	.0723	.0920
2010 Aug 05	1	2455413.919329	1.3131	1.4145	1.5159	1.1531	1.2499	1.3467	.0255	.0428	.0600
2010 Aug 05	2	2455413.937581	1.3324	1.4031	1.4739	1.1799	1.2473	1.3147	.0279	.0368	.0457
2010 Aug 05	3	2455413.957431	1.3509	1.4272	1.5036	1.1799	1.2527	1.3255	.0274	.0379	.0484
2010 Sep 24	1	2455463.808264	1.3908	1.4178	1.4447	1.2666	1.2890	1.3114	.0466	.0580	.0694
2010 Sep 24	2	2455463.825220	1.3890	1.4157	1.4424	1.2633	1.2868	1.3103	.0579	.0668	.0756
2010 Oct 08	1	2455477.790775	1.4504	1.4809	1.5115	1.3268	1.3547	1.3825	.0441	.0577	.0712
2010 Oct 08	2	2455477.811817	1.4598	1.4852	1.5106	1.3289	1.3502	1.3714	.0458	.0611	.0764
2010 Nov 04	1	2455504.728750	1.5895	1.6337	1.6778	1.4508	1.4897	1.5286	.0749	.0869	.0990
2010 Nov 04	2	2455504.741042	1.5957	1.6383	1.6809	1.4492	1.4899	1.5305	.0757	.0904	.1052
2010 Nov 04	3	2455504.753403	1.6113	1.6394	1.6675	1.4716	1.4981	1.5246	.0738	.0839	.0940
2010 Dec 07	1	2455537.779896	1.7500	1.7803	1.8105	1.6409	1.6664	1.6920	.0421	.0577	.0732
2010 Dec 07	2	2455537.792292	1.7341	1.7717	1.8092	1.6318	1.6595	1.6871	.0502	.0625	.0748
2010 Dec 07	3	2455537.803646	1.7448	1.7730	1.8011	1.6352	1.6591	1.6831	.0379	.0525	.0672
2010 Dec 25	1	2455555.738889	1.7719	1.8017	1.8316	1.6643	1.6941	1.7239	.0545	.0662	.0780
2010 Dec 25	2	2455555.750000	1.7458	1.8050	1.8641	1.6412	1.6910	1.7409	.0579	.0691	.0804
2011 Jan 17	1	2455578.718461	1.7408	1.7710	1.8012	1.6433	1.6676	1.6920	.1040	.1163	.1286
2011 Jan 17	2	2455578.737396	1.7401	1.7717	1.8033	1.6441	1.6675	1.6909	.1022	.1150	.1278
2011 Jan 27	1	2455588.685625	1.7520	1.7767	1.8014	1.6632	1.6888	1.7144	.1062	.1245	.1428
2011 Jan 27	2	2455588.697546	1.7641	1.8006	1.8371	1.6678	1.6981	1.7285	.0995	.1175	.1354

Table continued on following pages

Table 1. ε Aur, equivalent widths (in Ångstroms) and 95% confidence limits for Na D_2, Na D_1, and the 5853Å line, cont.

Date	*Spectrum Sequence Number*	*Julian Date*	*Na D_2 Lower Conf. Limit (Å)*	*Na D_2 EW (Å)*	*Na D_2 Upper Conf. Limit (Å)*	*Na D_1 Lower Conf. Limit (Å)*	*Na D_1 EW (Å)*	*Na D_1 Upper Conf. Limit(Å)*	*5853Å Lower Conf. Limit (Å)*	*5853Å EW (Å)*	*5853Å Upper. Conf. Limit (Å)*
2011 Feb 12	1	2455604.663553	1.7764	1.8215	1.8665	1.6841	1.7219	1.7597	.0839	.1003	.1166
2011 Feb 12	2	2455604.679606	1.7707	1.8058	1.8408	1.6762	1.7112	1.7462	.0892	.1117	.1341
2011 Mar 05	1	2455625.639016	1.8054	1.8575	1.9095	1.6769	1.7154	1.7538	.0831	.1004	.1177
2011 Mar 05	2	2455625.649919	1.8086	1.8605	1.9124	1.6883	1.7264	1.7645	.0830	.1009	.1188
2011 Mar 05	3	2455625.660567	1.8149	1.8650	1.9150	1.6978	1.7330	1.7681	.0835	.1015	.1195
2011 Mar 05	4	2455625.673125	1.8096	1.8655	1.9215	1.6950	1.7353	1.7756	.0855	.1021	.1187
2011 Mar 10	1	2455630.687222	1.8009	1.8610	1.9211	1.6704	1.7155	1.7606	.0674	.0899	.1125
2011 Mar 10	2	2455630.697222	1.7927	1.8554	1.9181	1.6679	1.7126	1.7573	.0655	.0822	.0989
2011 Mar 10	3	2455630.708461	1.8104	1.8574	1.9043	1.6786	1.7145	1.7504	.0696	.0856	.1015
2011 Mar 23	1	2455643.651956	1.8097	1.8647	1.9196	1.6626	1.7132	1.7638	.0511	.0682	.0852
2011 Mar 23	2	2455643.667616	1.8159	1.8716	1.9272	1.6648	1.7151	1.7654	.0718	.0972	.1225
2011 Mar 23	3	2455643.682164	1.8277	1.8646	1.9015	1.6772	1.7080	1.7388	.0521	.0714	.0908
2011 Apr 02	1	2455653.638958	1.7557	1.8112	1.8668	1.6099	1.6533	1.6966	.0500	.0638	.0776
2011 Apr 02	2	2455653.648762	1.7552	1.8082	1.8611	1.6081	1.6492	1.6904	.0440	.0621	.0802
2011 Apr 13	1	2455664.638056	1.7012	1.7541	1.8070	1.5599	1.5981	1.6362	.0630	.0786	.0941
2011 Apr 13	2	2455664.647801	1.7172	1.7612	1.8052	1.5774	1.6139	1.6503	.0705	.0830	.0954
2011 Apr 13	3	2455664.658252	1.7073	1.7650	1.8228	1.5643	1.6082	1.6522	.0587	.0777	.0967
2011 Apr 26	1	2455677.616528	1.6404	1.6810	1.7215	1.5047	1.5326	1.5605	.0746	.0841	.0936
2011 Apr 26	2	2455677.631076	1.6256	1.6646	1.7035	1.4984	1.5314	1.5643	.0711	.0847	.0983
2011 Apr 26	3	2455677.647581	1.6293	1.6761	1.7228	1.4956	1.5308	1.5660	.0728	.0834	.0940
2011 May 08	1	2455689.627975	1.6196	1.6586	1.6976	1.4791	1.5028	1.5265	.1022	.1113	.1205

Table continued on next page

Table 1. ε Aur, equivalent widths (in Ångstroms) and 95% confidence limits for Na D_2, Na D_1, and the 5853Å line, cont.

Date	Spectrum Sequence Number	Julian Date	Na D_2 Lower Conf. Limit (Å)	Na D_2 EW (Å)	Na D_2 Upper Conf. Limit (Å)	Na D_1 Lower Conf. Limit (Å)	Na D_1 EW (Å)	Na D_1 Upper Conf. Limit(Å)	5853Å Lower Conf. Limit (Å)	5853Å EW (Å)	5853Å Upper. Conf. Limit (Å)
2011 May 31	1	2455712.626944	1.5604	1.6194	1.6785	1.4383	1.4776	1.5169	.0830	.1014	.1198
2011 Aug 16	1	2455789.862280	1.2727	1.3440	1.4153	1.2160	1.2870	1.3581	.0661	.0850	.1040
2011 Aug 16	2	2455789.876863	1.2920	1.3635	1.4350	1.2244	1.2915	1.3586	.0696	.0787	.0877
2011 Aug 30	1	2455803.851956	1.2969	1.3255	1.3541	1.2218	1.2448	1.2678	.0283	.0402	.0521
2011 Aug 30	2	2455803.865093	1.2985	1.3229	1.3474	1.2259	1.2449	1.2638	.0312	.0429	.0546
2011 Sep 18	1	2455822.813137	1.2674	1.2931	1.3188	1.1765	1.1988	1.2212	.0300	.0402	.0505
2011 Oct 10	1	2455844.770972	1.1888	1.2073	1.2258	1.1119	1.1316	1.1513	.0440	.0519	.0599

Table 2. Standard deviations for line estimation methods.

Line	Method	Mean	Std Dev.
5853Å	EW Barycenter	5853.5185	0.24589
	EW Gaussian	5853.4722	0.31127
Na D_2	EW Barycenter	5889.7920	0.31523
	EW Gaussian	5889.8235	0.30328
	Visual Barycenter	5889.8086	0.30284
	Visual Gaussian	5889.8239	0.30320
Na D_1	EW Barycenter	5895.7780	0.30931
	EW Gaussian	5895.7966	0.30839
	Visual Barycenter	5895.7852	0.30721
	Visual Gaussian	5895.7969	0.30845

Table 3. ε Aur, line center estimates in Ångstroms for Na D_2, Na D_1, the 5853Å line, and the 5853Å split line.

Date	*Spectrum Sequence Number*	*Julian Date*	*Na D_2 (Å)*	*Na D_1 (Å)*	*5853Å Line (Å)*	*5853Å Split Line (Å)*
2010 Feb 13	1	2455240.719352	5890.1240	5896.1199	5853.6636	—
2010 Feb 13	2	2455240.740081	5890.1328	5896.1319	5853.6760	—
2010 Feb 13	3	2455240.762222	5890.1580	5896.1532	5853.6721	—
2010 Feb 14	1	2455241.686528	5890.1130	5896.1122	5853.6458	—
2010 Feb 14	2	2455241.712986	5890.1520	5896.1372	5853.6659	—
2010 Feb 14	3	2455241.734444	5890.1348	5896.1408	5853.6925	—
2010 Feb 19	1	2455246.633507	5890.1841	5896.1650	5853.7409	—
2010 Feb 19	2	2455246.651863	5890.1750	5896.1535	5853.7411	—
2010 Feb 19	3	2455246.669815	5890.1762	5896.1708	5853.7455	—
2010 Feb 19	4	2455246.680093	5890.1769	5896.1693	5853.7587	—
2010 Feb 26	1	2455253.654190	5890.1869	5896.1867	5853.7940	—
2010 Mar 04	1	2455259.650289	5890.2260	5896.2160	5853.9072	—
2010 Mar 04	2	2455259.669225	5890.1948	5896.1877	5853.8784	—
2010 Mar 04	3	2455259.689699	5890.2227	5896.2039	5853.8547	—
2010 Mar 13	1	2455268.681319	5890.2551	5896.2396	5853.8716	—
2010 Mar 13	2	2455268.702488	5890.2340	5896.2190	5853.8145	—
2010 Mar 13	3	2455268.722338	5890.2398	5896.2217	5853.9332	—
2010 Mar 28	1	2455283.653206	5890.2747	5896.2642	5853.6779	5853.7398
2010 Mar 28	2	2455283.674873	5890.2816	5896.2531	5853.7153	5853.7943
2010 Mar 28	3	2455283.695197	5890.2584	5896.2483	5853.7051	—
2010 May 08	1	2455324.636933	5890.2483	5896.2159	5853.7420	—
2010 May 08	2	2455324.647917	5890.2486	5896.2260	5853.8617	—

Table continued on following pages

Table 3. ε Aur, line center estimates in Ångstroms for Na D_2, Na D_1, the 5853Å line, and the 5853Å split line, cont.

Date	*Spectrum Sequence Number*	*Julian Date*	*Na D_2 (Å)*	*Na D_1 (Å)*	*5853Å Line (Å)*	*5853Å Split Line (Å)*
2010 May 08	3	2455324.658241	5890.2334	5896.2057	5853.8222	—
2010 Aug 05	1	2455413.919329	5889.9752	5895.9164	5853.4407	—
2010 Aug 05	2	2455413.937581	5889.9750	5895.9192	5853.4436	—
2010 Aug 05	3	2455413.957431	5889.9444	5895.9222	5853.4442	—
2010 Sep 24	1	2455463.808264	5889.7200	5895.7016	5853.6694	5853.6473
2010 Sep 24	2	2455463.825220	5889.7234	5895.7037	5853.6482	—
2010 Oct 08	1	2455477.790775	5889.6684	5895.6463	5853.4881	—
2010 Oct 08	2	2455477.811817	5889.6509	5895.6249	5853.4813	—
2010 Nov 04	1	2455504.728750	5889.5534	5895.5358	5853.4995	—
2010 Nov 04	2	2455504.741042	5889.5618	5895.5321	5853.5089	—
2010 Nov 04	3	2455504.753403	5889.5641	5895.5408	5853.5117	—
2010 Dec 07	1	2455537.779896	5889.5108	5895.4989	5853.5746	—
2010 Dec 07	2	2455537.792292	5889.5315	5895.5149	5853.5760	5853.6130
2010 Dec 07	3	2455537.803646	5889.5159	5895.4926	5853.5497	—
2010 Dec 25	1	2455555.738889	5889.5171	5895.4846	5853.2774	—
2010 Dec 25	2	2455555.750000	5889.5177	5895.4922	5853.2923	—
2011 Jan 17	1	2455578.718461	5889.4816	5895.4511	5853.3708	5853.5019
2011 Jan 17	2	2455578.737396	5889.4974	5895.4673	5853.3825	—
2011 Jan 27	1	2455588.685625	5889.5192	5895.4856	5853.5203	5853.3694
2011 Jan 27	2	2455588.697546	5889.4865	5895.4618	5853.4414	5853.4001
2011 Feb 12	1	2455604.663553	5889.5145	5895.4847	5853.3657	5853.2924
2011 Feb 12	2	2455604.679606	5889.5255	5895.4939	5853.4441	5853.2943

Table continued on following pages

Table 3. ε Aur, line center estimates in Ångstroms for Na D_2, Na D_1, the 5853Å line, and the 5853Å split line, cont.

Date	*Spectrum Sequence Number*	*Julian Date*	*Na D_2 (Å)*	*Na D_1 (Å)*	*5853Å Line (Å)*	*5853Å Split Line (Å)*
2011 Mar 05	1	2455625.639016	5889.5191	5895.5073	5853.3333	—
2011 Mar 05	2	2455625.649919	5889.5318	5895.5162	5853.3115	5853.2227
2011 Mar 05	3	2455625.660567	5889.5563	5895.5309	5853.3217	5853.2341
2011 Mar 05	4	2455625.673125	5889.5237	5895.4970	5853.3485	5853.1924
2011 Mar 10	1	2455630.687222	5889.5455	5895.5073	5853.2979	5853.2301
2011 Mar 10	2	2455630.697222	5889.5403	5895.5196	5853.3628	5853.2312
2011 Mar 10	3	2455630.708461	5889.5418	5895.5140	5853.3122	5853.2427
2011 Mar 23	1	2455643.651956	5889.5093	5895.4974	5853.1718	—
2011 Mar 23	2	2455643.667616	5889.5394	5895.5094	—	—
2011 Mar 23	3	2455643.682164	5889.5245	5895.5105	5853.2195	5853.3272
2011 Apr 02	1	2455653.638958	5889.5626	5895.5333	5853.0783	—
2011 Apr 02	2	2455653.648762	5889.5392	5895.5210	5853.0749	—
2011 Apr 13	1	2455664.638056	5889.5417	5895.5153	5853.0564	—
2011 Apr 13	2	2455664.647801	5889.5452	5895.5193	5853.0654	—
2011 Apr 13	3	2455664.658252	5889.5331	5895.5135	5853.0611	—
2011 Apr 26	1	2455677.616528	—	—	5853.1024	5853.0742
2011 Apr 26	2	2455677.631076	5889.5672	5895.5349	5853.1409	—
2011 Apr 26	3	2455677.647581	5889.5658	5895.5371	5853.1361	—
2011 May 08	1	2455689.627975	5889.5490	5895.5315	5853.2246	5853.1741
2011 May 31	1	2455712.626944	5889.6136	5895.6052	5853.4914	5853.1330
2011 Aug 16	1	2455789.862280	5889.8000	5895.7474	5853.8034	—
2011 Aug 16	2	2455789.876863	5889.8108	5895.7479	5853.7481	—

Table continued on next page

Table 3. ε Aur, line center estimates in Ångstroms for Na D_2, Na D_1, the 5853Å line, and the 5853Å split line, cont.

Date	*Spectrum Sequence Number*	*Julian Date*	*Na D_2 (Å)*	*Na D_1 (Å)*	*5853Å Line (Å)*	*5853Å Split Line (Å)*
2011 Aug 30	1	2455803.851956	5889.8141	5895.7765	5853.7714	—
2011 Aug 30	2	2455803.865093	5889.8313	5895.7729	5853.7397	—
2011 Sep 18	1	2455822.813137	5889.8196	5895.7627	5853.4599	5853.3919
2011 Oct 10	1	2455844.770972	5889.7865	5895.7378	5853.6354	—

Table 4. ε Aur, radial velocities (km/sec) for Na D_2, Na D_1, the 5853Å line, and the 5853Å split line (negative value = blue Doppler shift; positive value = red Doppler shift).

Date	*Spectrum Sequence Number*	*Julian Date*	*Na D_2 (Å)*	*Na D_1 (Å)*	*5853Å (Å)*	*5853Å Split Line (Å)*
2010 Feb 13	1	2455240.719352	8.856	10.164	2.233	—
2010 Feb 13	2	2455240.740081	9.304	10.774	2.868	—
2010 Feb 13	3	2455240.762222	10.587	11.857	2.668	—
2010 Feb 14	1	2455241.686528	8.296	9.773	1.321	—
2010 Feb 14	2	2455241.712986	10.281	11.044	2.351	—
2010 Feb 14	3	2455241.734444	9.406	11.227	3.713	—
2010 Feb 19	1	2455246.633507	11.915	12.457	6.192	—
2010 Feb 19	2	2455246.651863	11.452	11.873	6.202	—
2010 Feb 19	3	2455246.669815	11.513	12.752	6.427	—

Table continued on following pages

Table 4. ε Aur, radial velocities (km/sec) for Na D_2, Na D_1, the 5853Å line, and the 5853Å split line (negative value = blue Doppler shift; positive value = red Doppler shift), cont.

Date	*Spectrum Sequence Number*	*Julian Date*	*Na D_2 (Å)*	*Na D_1 (Å)*	*5853Å (Å)*	*5853Å Split Line (Å)*
2010 Feb 19	4	2455246.680093	11.549	12.676	7.103	—
2010 Feb 26	1	2455253.654190	12.058	13.561	8.911	—
2010 Mar 04	1	2455259.650289	14.048	15.050	14.709	—
2010 Mar 04	2	2455259.669225	12.460	13.612	13.234	—
2010 Mar 04	3	2455259.689699	13.880	14.435	12.020	—
2010 Mar 13	1	2455268.681319	15.529	16.250	12.885	—
2010 Mar 13	2	2455268.702488	14.455	15.203	9.961	—
2010 Mar 13	3	2455268.722338	14.750	15.340	16.040	—
2010 Mar 28	1	2455283.653206	16.526	17.501	2.965	6.135
2010 Mar 28	2	2455283.674873	16.878	16.937	4.881	8.927
2010 Mar 28	3	2455283.695197	15.697	16.693	4.358	—
2010 May 08	1	2455324.636933	15.183	15.045	6.248	—
2010 May 08	2	2455324.647917	15.198	15.559	12.378	—
2010 May 08	3	2455324.658241	14.424	14.527	10.355	—
2010 Aug 05	1	2455413.919329	1.283	–0.183	–9.183	—
2010 Aug 05	2	2455413.937581	1.272	–0.041	–9.034	—
2010 Aug 05	3	2455413.957431	–0.285	0.112	–9.004	—
2010 Sep 24	1	2455463.808264	–11.707	–11.105	2.530	1.398
2010 Sep 24	2	2455463.825220	–11.534	–10.998	1.444	—
2010 Oct 08	1	2455477.790775	–14.333	–13.917	–6.755	—

Table continued on following pages

Table 4. ε Aur, radial velocities (km/sec) for Na D_2, Na D_1, the 5853Å line, and the 5853Å split line (negative value = blue Doppler shift; positive value = red Doppler shift), cont.

Date	*Spectrum Sequence Number*	*Julian Date*	*Na D_2 (Å)*	*Na D_1 (Å)*	*5853Å (Å)*	*5853Å Split Line (Å)*
2010 Oct 08	2	2455477.811817	–15.224	–15.005	–7.104	—
2010 Nov 04	1	2455504.728750	–20.187	–19.536	–6.171	—
2010 Nov 04	2	2455504.741042	–19.760	–19.724	–5.690	—
2010 Nov 04	3	2455504.753403	–19.643	–19.282	–5.547	—
2010 Dec 07	1	2455537.779896	–22.356	–21.413	–2.325	—
2010 Dec 07	2	2455537.792292	–21.302	–20.599	–2.253	–0.359
2010 Dec 07	3	2455537.803646	–22.096	–21.733	–3.600	—
2010 Dec 25	1	2455555.738889	–22.035	–22.140	–17.547	—
2010 Dec 25	2	2455555.750000	–22.004	–21.753	–16.784	—
2011 Jan 17	1	2455578.718461	–23.842	–23.843	–12.763	–6.049
2011 Jan 17	2	2455578.737396	–23.038	–23.019	–12.164	—
2011 Jan 27	1	2455588.685625	–21.928	–22.089	–5.106	–12.835
2011 Jan 27	2	2455588.697546	–23.593	–23.299	–9.147	–11.262
2011 Feb 12	1	2455604.663553	–22.167	–22.135	–13.024	–16.778
2011 Feb 12	2	2455604.679606	–21.607	–21.667	–9.009	–16.681
2011 Mar 05	1	2455625.639016	–21.933	–20.985	–14.684	—
2011 Mar 05	2	2455625.649919	–21.287	–20.533	–15.800	–20.348
2011 Mar 05	3	2455625.660567	–20.040	–19.785	–15.278	–19.764
2011 Mar 05	4	2455625.673125	–21.699	–21.509	–13.905	–21.900
2011 Mar 10	1	2455630.687222	–20.589	–20.985	–16.497	–19.969

Table continued on next page

Table 4. ε Aur, radial velocities (km/sec) for Na D_2, Na D_1, the 5853Å line, and the 5853Å split line (negative value = blue Doppler shift; positive value = red Doppler shift), cont.

Date	*Spectrum Sequence Number*	*Julian Date*	*Na D_2 (Å)*	*Na D_1 (Å)*	*5853Å (Å)*	*5853Å Split Line (Å)*
2011 Mar 10	2	2455630.697222	–20.854	–20.360	–13.173	–19.913
2011 Mar 10	3	2455630.708461	–20.778	–20.645	–15.764	–19.324
2011 Mar 23	1	2455643.667616	–20.900	–20.879	—	—
2011 Mar 23	2	2455643.651956	–22.432	–21.489	–22.955	—
2011 Mar 23	3	2455643.682164	–21.658	–20.823	–20.512	–14.996
2011 Apr 02	1	2455653.638958	–19.719	–19.663	–27.744	—
2011 Apr 02	2	2455653.648762	–20.910	–20.289	–27.918	—
2011 Apr 13	1	2455664.638056	–20.783	–20.579	–28.866	—
2011 Apr 13	2	2455664.647801	–20.605	–20.375	–28.405	—
2011 Apr 13	3	2455664.658252	–21.220	–20.670	–28.625	—
2011 Apr 26	1	2455677.616528	–24.127	–23.462	—	–27.954
2011 Apr 26	2	2455677.631076	–19.485	–19.582	–24.538	—
2011 Apr 26	3	2455677.647581	–19.556	–19.470	–24.784	—
2011 May 08	1	2455689.627975	–20.411	–19.755	–20.251	–22.838
2011 May 31	1	2455712.626944	–17.123	–16.007	–6.586	–24.943
2011 Aug 16	1	2455789.862280	–7.635	–8.776	9.393	—
2011 Aug 16	2	2455789.876863	–7.085	–8.751	6.561	—
2011 Aug 30	1	2455803.851956	–6.917	–7.297	7.754	—
2011 Aug 30	2	2455803.865093	–6.042	–7.480	6.130	—
2011 Sep 18	1	2455822.813137	–6.637	–7.998	–8.200	–11.682
2011 Oct 10	1	2455844.770972	–8.322	–9.265	0.789	—

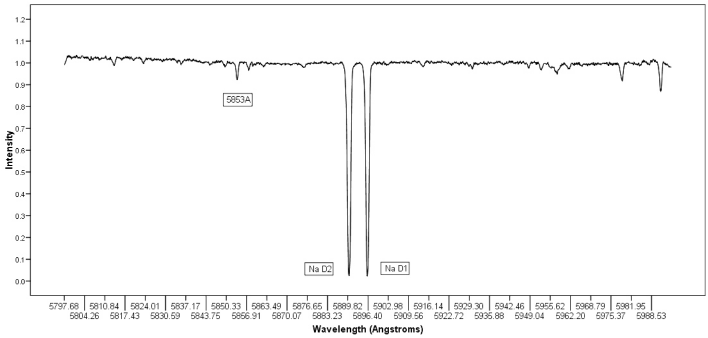

Figure 1. The sodium D lines region encompassing the 5853Å line. This is a normalized spectrum taken on February 26, 2010.

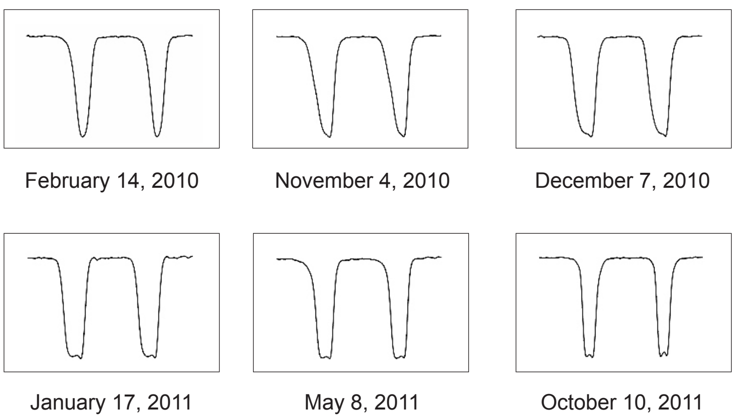

Figure 2. Example spectra to illustrate evolution of the sodium D lines.

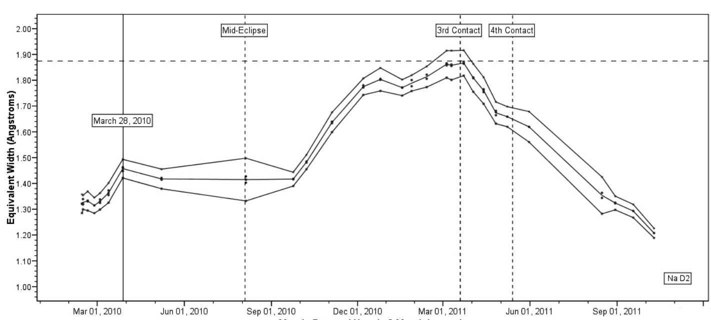

Figure 3. The sodium D_2 line equivalent widths (in Ångstroms) with upper and lower 95% confidence limits.

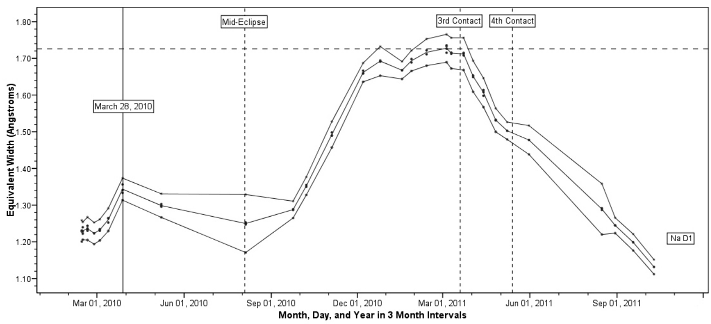

Figure 4. The sodium D_1 line equivalent widths (in Ångstroms) with upper and lower 95% confidence limits.

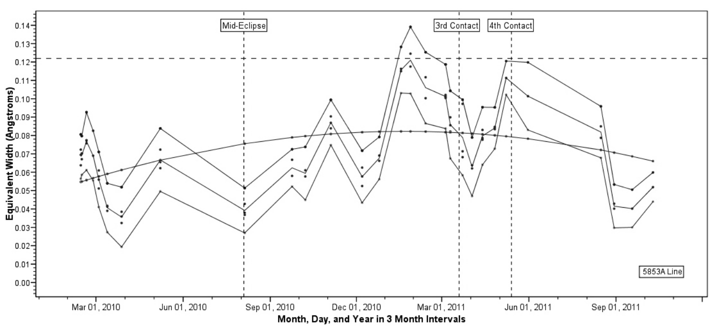

Figure 5. The 5853Å line equivalent widths (in Ångstroms) with upper and lower 95% confidence limits, and a superimposed second order polynomial regression line.

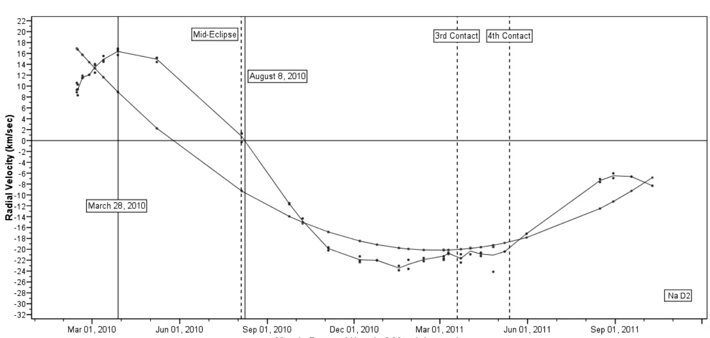

Figure 6. The sodium D_2 radial velocities (km/sec) and a superimposed second order polynomial regression line.

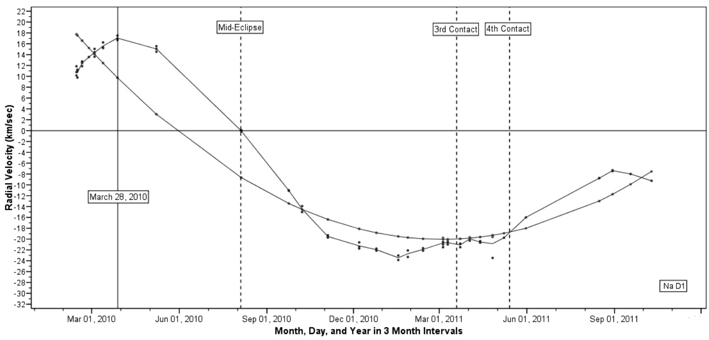

Figure 7. The sodium D_1 radial velocities (km/sec) and a superimposed second order polynomial regression line.

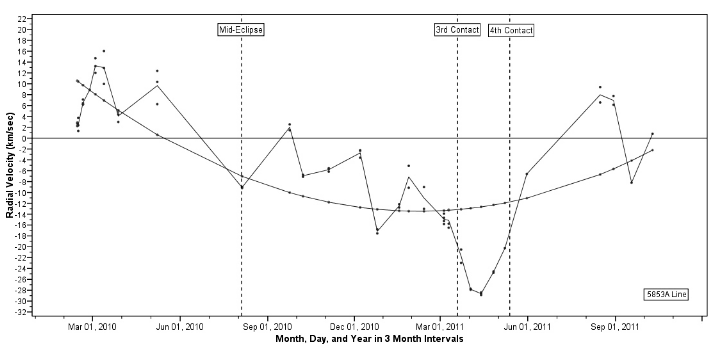

Figure 8. The 5853Å radial velocities (km/sec) and a superimposed second order polynomial regression line.

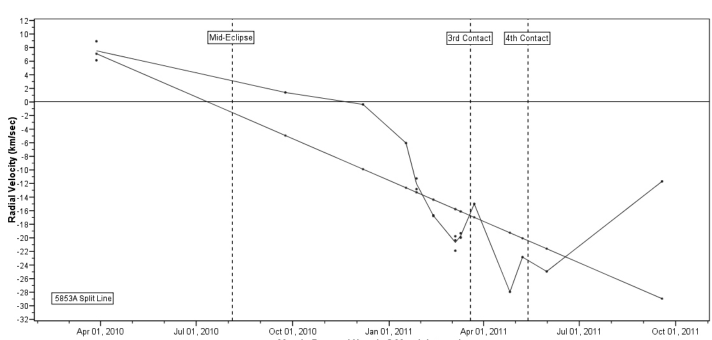

Figure 9. The 5853Å line radial velocities (km/sec) and a superimposed first order polynomial regression line.

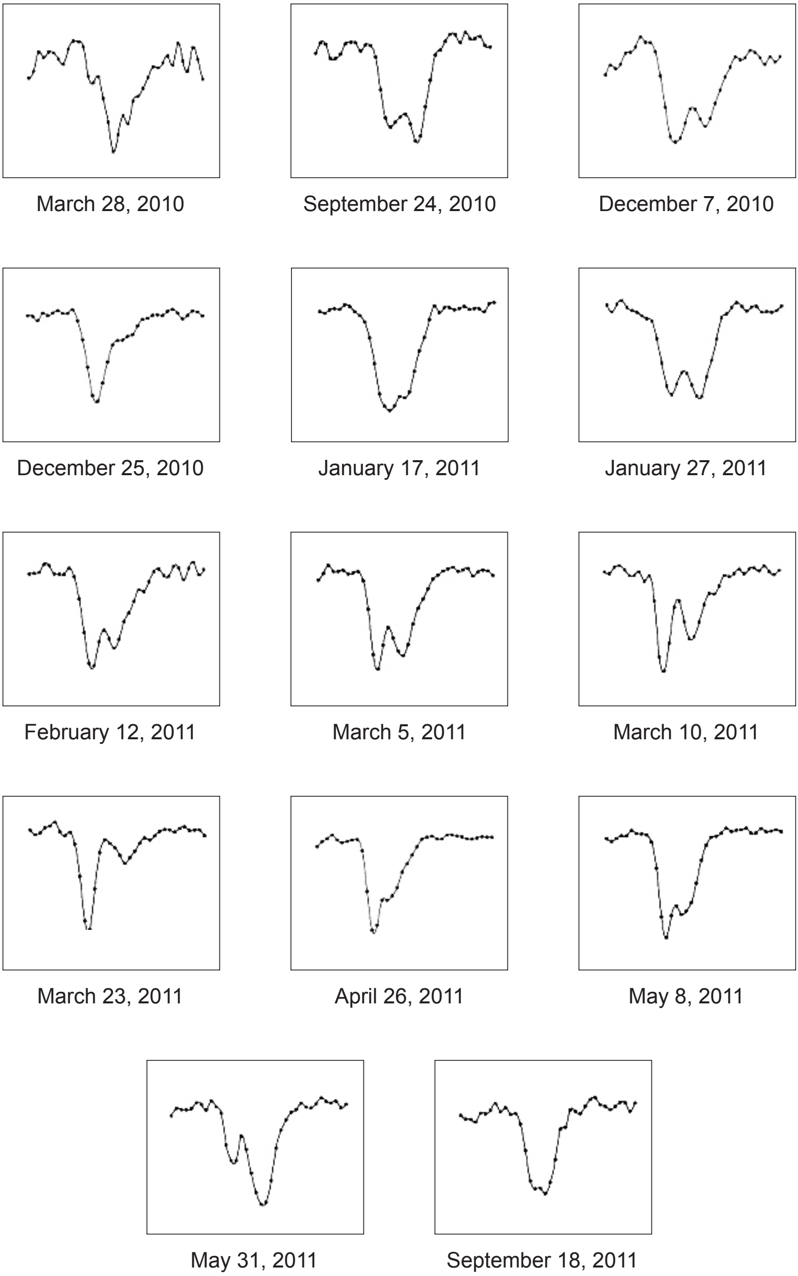

Figure 10. Evolution profiles of the 5853Å split line.